HUNTINGTON MEDICAL RESEARCH INSTITUTES

NEUROLOGICAL RESEARCH LABORATORY
734 Fairmount Avenue
Pasadena, California 91105

Contract No. NO1-NS-5-2333
QUARTERLY PROGRESS REPORT
January 1 - March 31, 1997

Report No. 6

"MICROSTIMULATION OF THE LUMBOSACRAL SPINAL CORD"

William F. Agnew, Ph.D.
Randy R. Carter, Ph.D.
Albert Lossinsky, Ph.D.
Douglas B. McCreery, Ph.D.
Leo A. Bullara, B.A.

This QPR is being sent to you before it has been reviewed by the staff of the Neural Prosthesis Program.

Abstract

Two chronic experiments were completed in the quarter and a third initiated. Our main goals were to evaluate the potential of modifying our microelectrode arrays by 1) reducing the electrode diameter, 2) using a straight versus coiled lead wire, and 3) using a 25 μm diameter lead wire rather than a 50 μm diameter lead wire. In addition, we sought to evaluate a new surgical implant procedure. While the number of experiments is as yet too small to be conclusive, physiologic results indicate that the new arrays may be implanted successfully but may fail mechanically within a few weeks. This may be due either to the mechanical properties of the electrodes and lead wires (e.g., thinner insulation, lower tensile strength, etc.) or may point to changes that need to be made in handling the arrays during surgery.

Comparative histological analysis of two animals in this quarter demonstrate significant movement and relocation of the electrodes, 50 days (SP-73) and one year (SP-59) after electrode implantation. Because of the apparent electrode shifting from one position to another, considerable scarring of the gray and white matter was observed by light microscopy in both animals. Remarkable changes in the regions of scarring include vascular hyperplasia, formation of reactive astrocytes, foamy cell phagocytes, and a considerable inflammatory response (SP-59). It is suggested that reinjury of the CNS by the occasional electrode movements may have contributed to the inflammatory lesions as a result of periodic antigen exposure from the injured tissues.

Introduction

The overall goals of this contract are to develop a method of chronic microstimulation of the sacral cord of the cat to effect micturition, and to evaluate the effects of the electrical stimulation on neural and surrounding tissues. In this report we discuss the results from three chronic experiments in which microelectrodes were implanted in the sacral spinal cord.

In the first two cases (SP-74 and SP-75), the implants failed mechanically. In SP-74, the failure may have been unrelated to the microelectrode array but was due instead to gross failure of the external stabilization pad to isolate the delicate lead wires from movement-induced stress. The mode of failure of SP-75 is still under investigation. The third experiment (SP-76) is ongoing.

Histologic results are described from two experiments. The first (SP-59) is a chronic experiment in which the microelectrode array did not produce evoked potentials or bladder pressure elevation sufficient to provide a basis for our chronic stimulation paradigm. Instead, this animal was followed for more than one year to provide an example of the response of the cord to such a long-term microelectrode implantation. In a more recent experiment (SP-73) we report our findings on an animal in which the spinal cord was stimulated for a 12 hour period on each of 2 successive days.

Methods

Adult male cats were anesthetized with 50% nitrous oxide and 1-2% Halothane and the spinal cord exposed as described previously. The S_2 region of the spinal cord was localized by stimulation of the dermatome it serves while recording the dorsal cord potential supradurally, as described previously. Four activated iridium microelectrodes (24-50 μm dia., 2.8 mm long, 2000 μm^2 exposed stimulating surface) were implanted manually at approximately the dorsal midline of the spinal cord and angled laterally at about 10 degrees. No matrix was used to support the electrodes. The electrodes were pulsed individually and the bladder lumen pressure was monitored. The electrodes were advanced into the cord until good elevation of bladder pressure was produced by the stimulation. The dura was then closed over the electrodes and the effect of the stimulation again measured. A silastic pad (to which the stimulating electrode leads had been glued) was sutured to the dura to reduce traction on the electrodes. The ground (indifferent) electrode was sutured in place over the microelectrodes. A small hole was made in the dura and a recording electrode inserted so as to lie approximately 3 cm caudal to the stimulating electrodes. A suture was used to secure the recording electrode to the dura. A reference electrode was sutured to the muscle 2 cm above the dura. The wound was flushed with antibacterial solution and the muscle and skin were closed in layers. Subsequent recordings were made with the animal anesthetized with Pentothal (i.v., as needed) or Nembutal (i.v., as needed). A sterile catheter and sterile saline were used during recording of the bladder lumenal pressure.

Within 20 minutes of the end of an experiment the animal was anesthetized with Nembutal and perfused through the aorta with saline followed by 2 L of ½ strength Karnovsky's fixative (2% paraformaldehyde and 2.5% glutaraldehyde) in 0.1 M sodium cacodylate buffer, pH 7.4. With the electrodes *in situ*, the complete cord and spinal roots were dissected out to precisely localize the microelectrodes. Two-mm-thick transverse sections containing the electrode tracks were dissected, processed and embedded in epoxy resin. One-μm thick sections were cut serially through the blocks and examined using light microscopy.

After tissue removal and location of the platinum plates (Fig. 1a), electrodes were identified (Fig. 1b). The precise location of the electrodes within the S_1-S_2 spinal cord was facilitated by carefully dissecting the spinal roots of the lumbar and sacral spinal cord. The electrodes with approximately 0.5 cm of cables were removed and placed into glycerol for scanning electron microscopic analysis. The spinal cord section containing the electrode tracks was sliced by hand into 1- 1.5 mm blocks, post-fixed with osmium tetroxide, dehydrated, and embedded in epon. One-μm thick, toluidine-blue stained sections were examined by light microscopy.

Results

Physiologic results. Two chronic experiments have been completed and a third initiated during this quarter. Our main goals were to reduce the diameter of the microelectrodes (our standard diameter is 50 μm) and to modify our surgical and implantation procedures.

In SP-74, a four electrode array was implanted. This array consisted of 34 μm diameter, activated Iridium electrodes with straight (rather than coiled) 25 μm diameter platinum leads. The standard surgical procedure was used (single 1.5 cm incision closed over the electrodes with continuous 7-0 suture). All electrodes had appropriate access resistances at the end of the surgery indicating their mechanical integrity. For our purposes, we consider access resistances 0-10 kΩ to be damaged, 10-20 kΩ to be marginal, 20-100 kΩ to be good, and above 100 kΩ to be damaged. Electrodes 2, 3, and 4 were electrically good at 6 days post-implant and electrode 1 was marginal. Stimulation of the spinal cord via the electrodes produced no bladder pressure elevations or somatic movements. A seroma appeared along both sides of the incision and was drained. Culture of a sample of the fluid removed showed no significant infection. At 13 days post-implant, only electrode 3 was electrically good, while the impedances in others were too high. This electrode elicited contraction of leg muscles. At 42 days post-implant, all the electrodes had high access resistances.

At 64 days post-implant, a dissection was performed prior to perfusion. The internal stabilization pad (without sutures indicating that they had become untied or pulled through the silastic pad) was just beneath the skin with the electrode leads severed distally. The external stabilization pad retained its sutures but was not connected to the fascia below. It is believed that the sutures of the external stabilization pad pulled through the underlying tissue removing strain relief on the smaller internal stabilization pad which then pulled through the sutures holding it to the dura and severing the delicate 25 µm lead wires.

In SP-75, a four electrode array was implanted. The electrodes consisted of 24 µm diameter, activated iridium electrodes with straight 25 µm diameter platinum leads. When initially implanted, the electrodes were all electrically good. The surgery consisted of a 1.5 cm incision but in this case the lead wires were grasped with padded forceps and pushed under the dura for several mm in an attempt to provide better strain relief. The incision was then closed as usual using continuous 7-0 suture. At this point, electrodes 1 and 3 were damaged (access resistance too low) while electrodes 2 and 4 were electrically good.

At 8 days post-implant, electrodes 2 and 4 remained electrically good, electrode 1 was marginal, and electrode 3 was damaged. Good evoked responses were obtained from stimulation of electrodes 2 and 4. Stimulation of electrode 4 (80 µA, 400 µs/ph, 32 nC/ph, ~~3,200~~ 1,600 µC/cm², 20 Hz, 1 s on, 2 s off) produced a significant elevation of bladder pressure with some voiding. Stimulation of electrodes 2 and 4 produced approximately twice the voided volume.

At 22 days post-implant, all electrodes were very low or marginal in access resistance. An evoked response was elicited by electrode 4 only and this consisted primarily of emg activity. Electrode 4 produced a weak, transient bladder pressure elevation at this time. A seroma with a light staph infection appeared at this point but resolved upon draining. A dissection prior to perfusion is planned to try to determine the cause of implant failure.

In SP-76, a four electrode array of the same design as that implanted into SP-75 was implanted. In this case, however, a very short (~ 1.5 mm) dural incision was made for each electrode. The lead was then bent into a "U" with padded forceps and the lead inserted through the opening. The electrode was then inserted into the cord with the result that approximately 8-10 mm of lead wire was below the dura. After all electrodes had been inserted through their individual openings, fibrin glue was used to seal the top of the dura. The advantage of this procedure is that the incisions are so small that CSF leakage is minimized and the dura/spinal cord does not "deflate." At the end of the surgery, all the electrodes were electrically good.

In this particular case, we had a difficult time maintaining the core temperature of the cat during surgery. Typically, the temperature is approximately 96 C during surgery (down from the cat's normal 101-102 C). However, here the core temperature during surgery was ~ 90-92 C despite a heating pad and radiant heat lamps. As expected, this animal did not eat well for several days after the surgery and was slow to walk. In approximately 5 days the cat appeared to be back to normal.

At 7 days post-implant, electrode 3 had a high access resistance. Evoked potentials were elicited by stimulation of electrodes 1 (mostly emg) and 4 (early response). Electrodes 1 and 2 had low somatic thresholds (25 and 49 μA, respectively) and seemed to activate the anal sphincter. This may indicate that the electrode stimulation sites are shallow and median to the bladder parasympathetic preganglionic nucleus. At 14 days post-implant, bladder contraction was obtained by pulsing electrode 1 (80 μA, 400 μs/ph, 32 nC/ph, ~~3,200~~ 1,600 μC/cm^2, 20 Hz, 1 s on, 2 s off) and a smaller contraction by pulsing electrode 4. Interleaved stimulation of electrodes 1 and 4, produced a significant bladder contraction but no voiding occurred.

TABLE I

SP #	TYPE STUDY	ELECTRODE #/SIZE	PULSED/UNPULSED	COMMENTS
SP-59	Chronic (one year)	1/ 50 µm	All Unpulsed	Histology completed
		2 / 50 µm		
		3 / 50 µm		
		4 / 50 µm		
SP-73	Chronic (50 days)	1 / 50 µm	Pulsed	Histology completed
		2 / 50 µm	Unpulsed	
		3 / 50 µm	Pulsed	
		4 / 50 µm	Unpulsed	
		5 / 38 µm	Passive	
		6 / 38 µm	Passive	
SP-74		1 / 32-34 µm	Unpulsed	Histology Incomplete
		2 / 32-34 µm	Unpulsed	
		3 / 32-34 µm	Unpulsed	
		4 / 32-34 µm	Unpulsed	
SP-75		1 / 24 µm	Unpulsed	Histology Incomplete
		2 / 24 µm	Unpulsed	
		3 / 24 µm	Unpulsed	
		4 / 24 µm	Unpulsed	
SP-76		1 / 24 µm	Unpulsed	Histology Incomplete
		2 / 24 µm	Unpulsed	
		3 / 24 µm	Unpulsed	
		4 / 24 µm	Unpulsed	

<u>Histologic Results (SP-59).</u>

In this quarter, histological evaluations were performed on SP-73 and SP-59, the latter animal was implanted over one year previously (February 12, 1996), as presented in TABLE I.

Gross observations. In both animals, only the S_1-S_2 spinal cord regions were evaluated. Analysis of control tissue from the cervical spinal cord was also performed. The tower, cables and stabilization pads remained within the animals. Good reossification of the spinal cord was observed in SP-59. A portion of the electrical cable was embedded within the bony overgrowth of the lumbar region of the spinal cord. Fig. 1a demonstrates the positioning of the platinum plate. The electrode beads are shown directly under the platinum plate (Fig. 1b).

Light microscopic observations. Three-dimensional, serial thick-section analysis was performed on the five plastic tissue blocks (A-E) that previously contained the electrodes. Although we expected to see the tips of electrodes 1 and 3 in the left hemisphere and electrodes 2 and 4 in the right hemispheres, based on the original surgical procedures, none of the four electrode tips was located in either the right or left, dorsal or ventral gray horns. Although the tips of electrodes 2 and 4 were not located within a specific cord region, the tip of electrode 4 was probably located within the right dorsal gray region (Fig. 2). Electrodes 1 and 2 and also electrodes 3 and 4 appeared to crisscross each other, while the track made by electrode 3 extended from the dorsal to ventral surfaces of this left hemisphere in block D. The capsules that encircled the electrodes was composed of several cell layers and appeared to be considerably thickened (Figs. 2,3).

An area of edema extended within blocks A-C forming a three-dimensional, cigar-shaped structure. This "zone of edema" was positioned dorsal to the central canal and is contrasted with a "normal" central canal region from the remote cervical spinal cord for comparison (Figs. 4-6). There was no histological evidence of electrode tracks in the vicinity of this zone of edema. Examining a distant portion of the spinal cord such as the cervical region serves as a useful control tissue and can indicate whether the tissue region in question is a generalized histopathological phenomenon, perhaps owing to a technical artifact, or if it is related to a local condition.

Remarkable pathological features adjacent to electrode tracks included a large inflammatory infiltrate that contained various leukocytes including monocytic cells, smaller, round lymphocytes, reactive astrocytes and scattered foamy cell macrophages (Figs. 7,8). Vascular hyperplasia was also observed within the scarred zones and surrounding the thickened capsules of the electrode tracks. Little neuronal chromatolysis of Nissl bodies was observed in neurons adjacent to tissue injury.

Summary. This animal was examined more than one year after electrode implantation. Spine ossification enclosed the electrode cables seemingly providing added stability to the cables. The thickened electrode capsule formation in addition to the strong perivascular infiltrate adjacent to the electrode capsules suggests that these processes were chronic rather than an acute response to the electrode presence within the tissue. No significant neuronal changes were noticed within neurons adjacent to electrodes except minor Nissl chromatolysis of some neurons.

Histologic results (SP-73). This animal was also described in the previous QPR # 5.

Gross observation. The electrodes appeared to be within the normal position after removal of the platinum plate.

Light microscopic observations. All six electrode tracks were identified, but only two electrode tips were located (Fig. 9).

In this case, considerable damage caused by electrode shifting was observed. Considerable hemorrhagic scarring was observed in many regions of the spinal cord where the electrodes appeared to have changed positions. This was pronounced in the vicinity of electrode 5 because of the extensive vascular hyperplasia and apparent final dorsal resting position of this electrode (Figs. 10,11). Torsion of the spinal cord was observed in some of the six plastic-embedded tissue blocks examined (Fig.12). Another electrode penetrated and disrupted the central canal altering the normal ependymal cell layer and surrounding tissue (Figs.13-15). Other pathological features included the cellular composition of the capsules surrounding the electrodes including stellate fibroblasts intermixed with collagen bundles and reactive astrocytes. A leukocytic inflammatory infiltrate was not observed in this animal despite the severe damage in the cord. Other phagocytic cells were noticed, especially Kolmer cells within the vicinity of the damaged ependymal cell layer of the central canal (Fig. 15). Although severe cord damage was apparent, little neuronal damage was observed bordering the injured tissue regions. Neuronal changes included minimal chromatolysis of the Nissl bodies. It was not possible to differentiate tissue changes between pulsed and unpulsed electrodes since we were unsure of precise locations of electrode tips in this animal.

Summary. Electrode movement was a major finding in this animal, but without an associated leukocytic infiltrate. In one tissue block examined, damage to the central canal was observed but without evidence of nearby electrodes. The explanation for this pathological zone of edema was not determined. Compared to SP-59, capsules surrounding the electrodes in this case were considerably thinner and consisted of stellate fibroblastic cells and collagen bundles.

Discussion

Two chronic experiments were completed in the quarter and a third initiated. Our main goals were to evaluate the potential of variously modifying our microelectrode arrays. Our initial results indicate that the arrays do not maintain sufficient integrity for periods longer than two to three weeks. It is unclear whether these results indicate that the scale of the electrodes or lead wires is too small to withstand the mechanical stresses of chronic implantation or whether our implantation procedure needs to be modified further to offer special protection to the more delicate arrays. We will conduct additional implants of similar design in the next quarter to address this issue.

We also evaluated a new surgical implant procedure. This procedure involves making small (~1.5 mm) slits in the dura rather than an extensive (~1.5 cm) opening. The advantage is that these small slits are not of sufficient size to cause the total loss of CSF pressure. As a result, the dura remains inflated and the spinal roots in their approximately normal position. After implantation, the slits were closed with fibrin glue rather than sutures. The hope is that such a procedure will reduce the possible movement of the electrodes as the dura is sutured closed. However, the tradeoff is a slightly more difficult and time consuming implantation procedure. The histologic results have not yet been obtained to allow evaluation.

Histological results of SP-59 and SP-73 demonstrate dramatic pathological consequences when electrodes become repositioned during normal back bending movements of the animals. The initial electrophysiological recordings in both animals indicated proper electrode implantation at the time of surgery. The remarkable and atypical pathology in addition to the failure to precisely locate many of the electrode tips support the idea of post-surgical electrode movement. This idea is further strengthened by the thickened electrode capsules observed in SP-59, in which the electrodes had been implanted for more than one year. Electrode movement could result in reinjury to the cord and, thus, periodically expose the animal to autoantigenic proteins. The heavy perivascular cuffing composed of mostly monocytic cells offers further support for such an hypothesis. Leukocytes are known to secrete cytotoxic compounds once they enter the tissues that could produce significant injury to neuronal and glial cell populations. Moreover, it is also possible that the unusually thickened capsules could have formed as a down growth of pial cells. It is also curious that, in light of the apparent serious damage to the spinal cord presented here, little neuronal damage was observed. Because we were not certain of the precise locations of electrode tips for any of the electrodes, it was not possible to comment on possible variability in histological changes that may occur between pulsed and unpulsed electrodes. Finally, the absence of perivascular swelling in blood vessels of the pericentral canal region in control spinal cord tissue indicated that the edema noted in the S_1-S_2 spinal cord is a reflection of electrode-associated injury (suspected movement) and not a result of increased pressure during vascular perfusion (technical artifact).

Future Work

In the next quarter we plan to conduct experiments in which the intensity of the chronic stimulation is increased. Past experiments have shown that chronic stimulation at functional levels of stimulation have been well tolerated by the cord. The goal of this next series of experiments is to determine the threshold of stimulation-induced neural damage. We also plan to implant chronic arrays of smaller electrodes (32 and 20 μm diameter) with the objective of minimizing mechanical damage to the cord.

Our histological studies set the framework to perform cytochemical studies for both qualitative and quantitative assessments of cellular damage observed in the spinal cord after electrode implantation. Such efforts could contribute to our overall understanding of the cellular types and changes that occur during and after electrical stimulation of the spinal cord, as well as indicating subtle injury that may occur in neurons and other cell types as a result of electrode movement. Such an approach may be useful in light of the fact that the application of cytochemical markers is usually considered as a more sensitive indicator of neuronal, glial and vascular changes that we may not be able to glean from basic histological techniques alone. In the next quarter, we plan to use special fixative schedules employing weaker aldehyde concentrations in order to properly preserve cellular enzymes and proteins for cytochemical and immunocytochemical studies. These studies will include identification of neuronal injury, leukocyte subtypes, and the disposition of the blood-brain barrier permeability in electrode implanted animals.

Fig. 1a. The platinum plate covering the electrodes below is shown with a slight diagonal shift.

Fig. 1b. Electrodes 1-4 are shown in this micrograph with cables intact.

Fig. 2. SP-59. Note the near crisscross pattern of the two electrode tracks made by electrodes 3 (*) and 4 (**). Electrode track 3 has penetrated the ventrolateral cord (arrowheads). Bar = 8.84 µm.

Fig. 3. SP-59. This is a higher magnification of Fig. 2. Note the thickened capsule formed by electrodes 3 (*) and 4 (**). Bar = 8.5 µm.

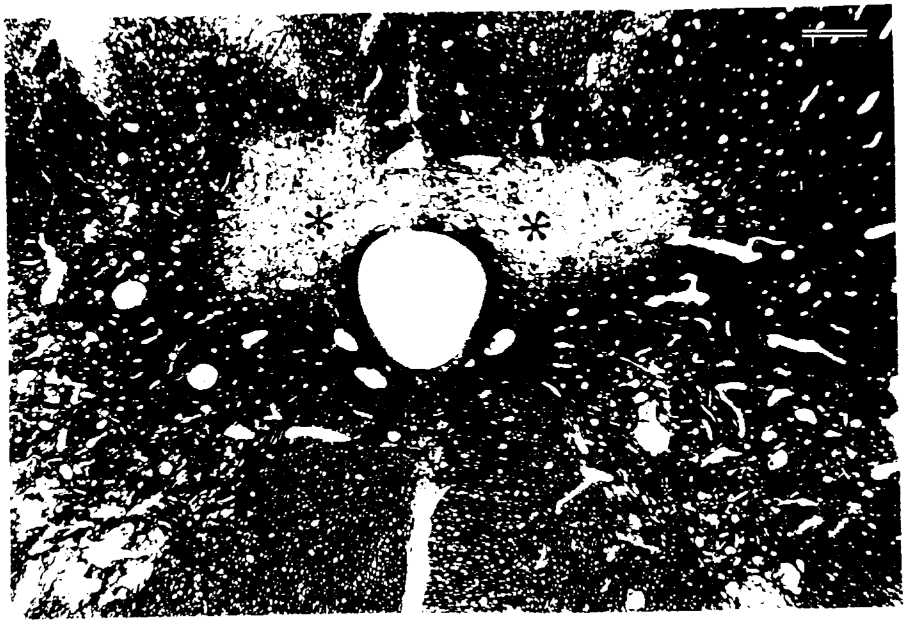

Figs. 4. SP-59. These micrographs demonstrate the severe edematous neuropil surrounding the dorsal portion of the central canal (*). In Fig. 5, note the myelinated figures within the vascular walls (arrowheads). One area of the ependymal cell region appears to be damaged (arrow). Bar = 8.5 μm.

Fig. 5. SP-59. Refer to Figure 4 for legend. Bar = 8.5 μm.

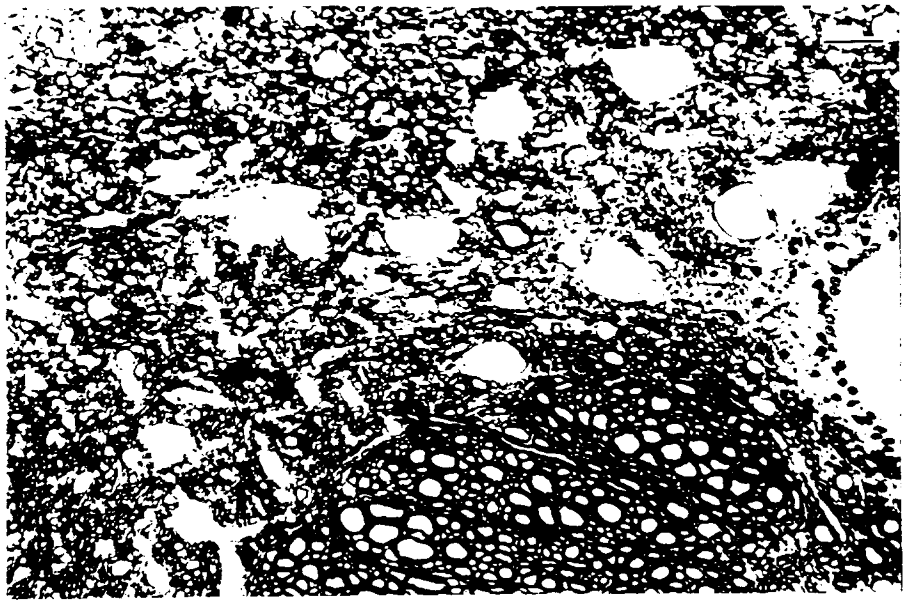

Fig. 6. SP-59, normal cervical spinal cord. This micrograph depicts the normal appearance of the central canal from control tissue distant for the electrode implantation. Because there is little perivascular edema in this tissue, this indicates that the perivascular edema is related to the injury within the S_1-S_2 region, and not to perfusion pressure during vascular fixation. Bar = 8.5 µm.

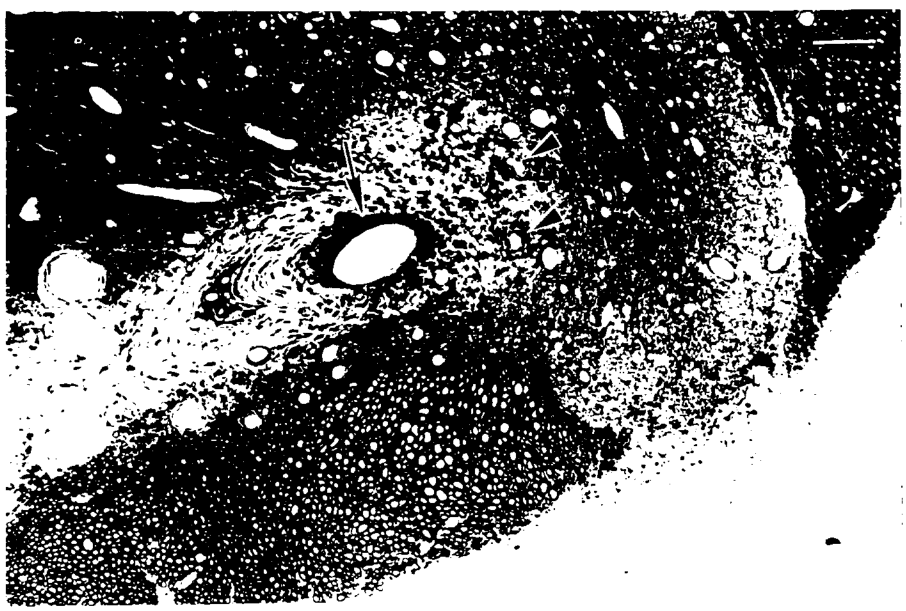

Fig. 7. SP-59. Panoramic view showing a portion of the track made by electrode 2. Note the thickened capsule (arrow) and perivascular cuffs (arrowheads). Bar = 8.5 µm.

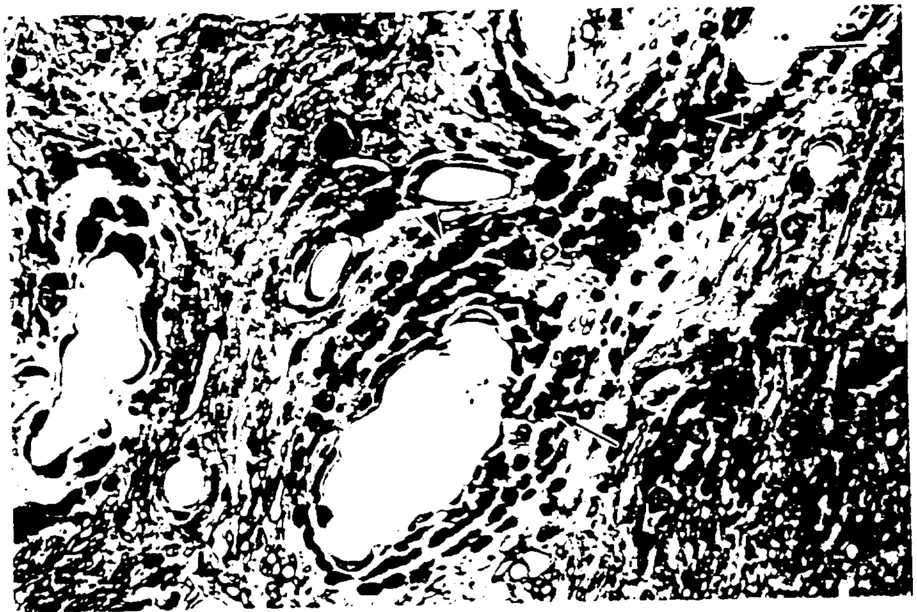

Fig.8. SP-59. This is a higher magnification from Fig. 7, demonstrating the leukocytic perivascular infiltrate composed primarily of small lymphocytes (arrows), mononuclear cells (arrowheads) and a few phagocytic cells (*). Bar = 8.5 µm.

Fig. 9. SP-73. In this panoramic view of the S_2 spinal cord, the region near the electrode tip is shown (arrowhead). Bar = 8.84 µm.

Fig. 10. SP-73. The track made by electrode 5 (arrowheads) appears to have moved to the dorsal resting position shown in this panoramic view. Note the prominent vascular hyperplasia presumably produced in response to the movement of the electrode. Bar = 8.84 µm.

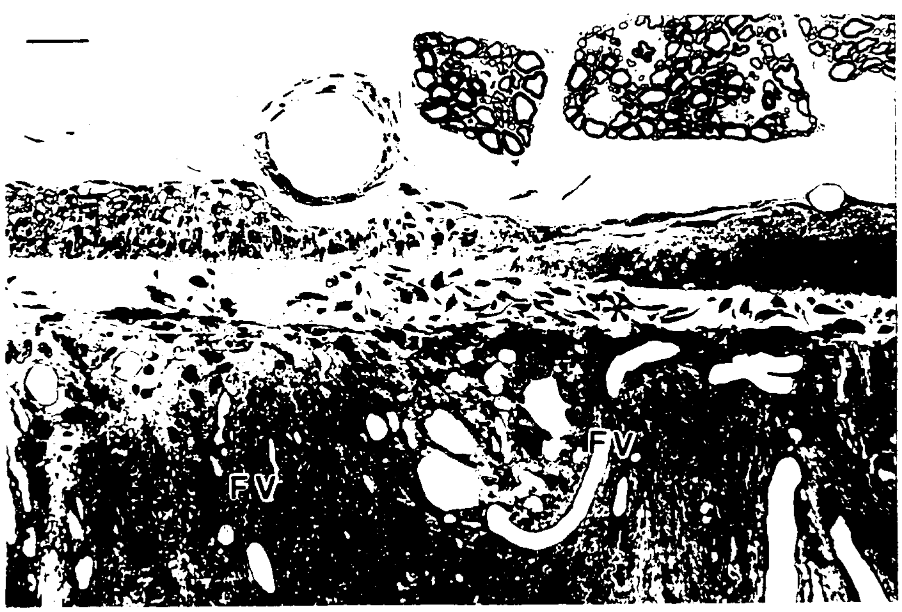

Fig. 11. SP-73. Higher magnification of Fig. 10 shows numerous stellate cells within the electrode track (*), adjacent to fibrovascular tissue (FV). Bar = 8.5 µm.

Fig. 12. SP-73. This micrograph depicts vascular hyperplasia (*) within the left hemisphere, that appears slightly contorted. Bar = 8.84 μm.

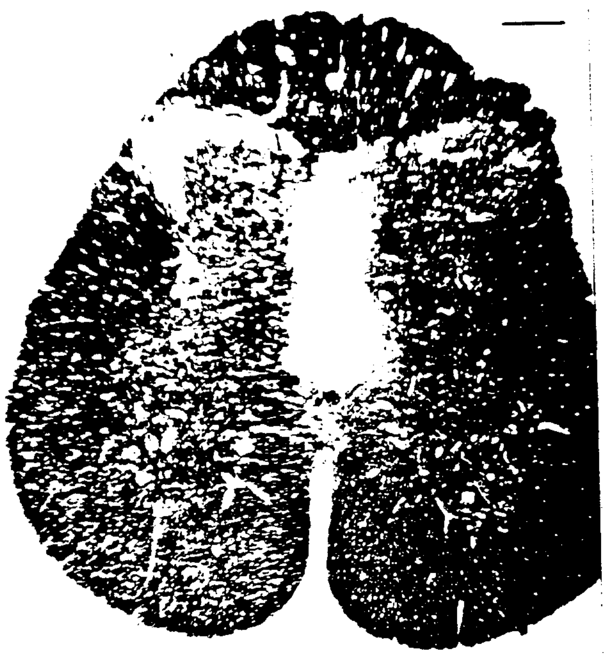

Fig. 13. SP-73. Electrode 6 penetrated the central canal (*). Note the edematous region surrounding the central canal. Bar = 8.5 μm.

Fig. 14. SP-73. Higher magnification from the damaged central canal is shown. Note the normal-appearing ependymal cells (*) adjacent to injured cells that have lost their structured integrity (arrowheads). The edematous neuropil is thought to be in part related to the breach in the epithelial cell layer. Bar = 8.5 µm.

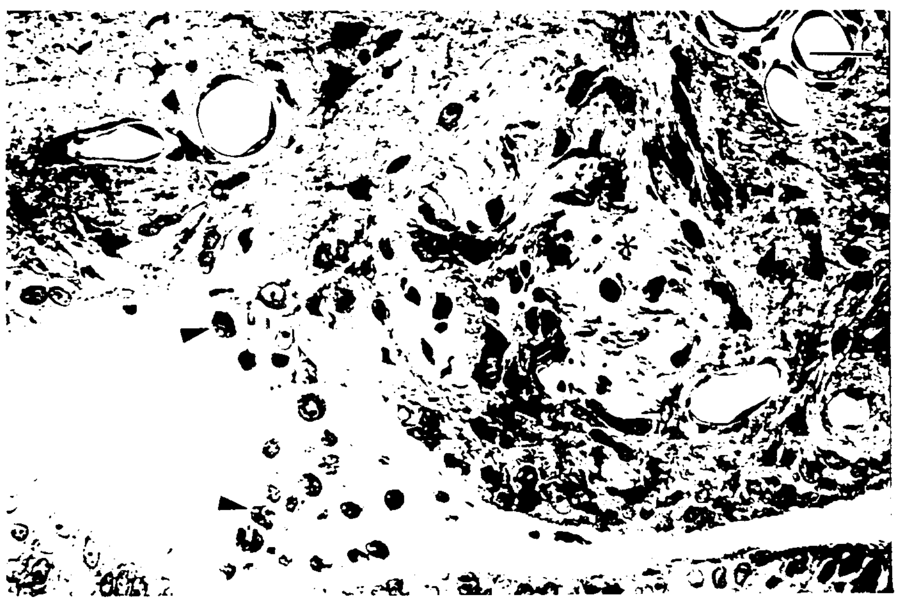

Fig. 15. SP-73. Another region of the damaged central canal is shown. Note the Kolmer cells (arrowheads) within the central canal space. These phagocytic cells play an important role in removing cellular debris. Note also the scarred area with reactive astrocytes (*). Bar = 8.5 µm.